NASA Technical Memorandum 88869

Cruise Noise of Counterrotation Propeller at Angle of Attack in Wind Tunnel

James H. Dittmar
Lewis Research Center
Cleveland, Ohio

October 1986

NASA

CRUISE NOISE OF COUNTERROTATION PROPELLER AT ANGLE OF ATTACK IN WIND TUNNEL

James H. Dittmar
National Aeronautics and Space Administration
Lewis Research Center
Cleveland, Ohio 44135

SUMMARY

The noise of a counterrotation propeller at angle of attack was measured in the NASA Lewis 8- by 6-Foot Supersonic Wind Tunnel at cruise conditions. Noise increases of as much as 4 dB were measured at positive angles of attack on the tunnel side wall, which represented an airplane fuselage. These noise increases could be minimized or eliminated by operating the counterrotation propeller with the front propeller turning up-inboard. This would require oppositely rotating propellers on opposite sides of the airplane. Noise analyses at different bandwidths enabled the separate front- and rear-propeller tones, as well as the total noise, at each harmonic to be determined. A simplified noise model was explored to show how the observed circumferential noise patterns of the separate propeller tones might have occurred. The total noise pattern, which represented the sum of the front- and rear-propeller tones at a particular harmonic, showed trends that would be hard to interpret without the separate-tone results. Therefore it is important that counterrotation angle-of-attack noise data be taken in such a manner that the front- and rear-propeller tones can be separated.

E-3275

INTRODUCTION

The noise generated by advanced fuel-conservative turboprops may create a cabin environment problem under cruise conditions. This noise may increase when the propellers are operated at angle of attack. Such increases have been observed on a subsonic single-rotation propeller by Tanna (ref. 1) and have been measured at cruise conditions for supersonic-tip-speed single-rotation propellers in the NASA Lewis 8- by 6-Foot Supersonic Wind Tunnel (refs. 2 and 3). The angle-of-attack noise of a counterrotation propeller at takeoff conditions has been measured by Block (ref. 4).

To evaluate how angle of attack affects the noise from a counterrotation advanced propeller at cruise, the F7-A7 counterrotation propeller model was tested in the Lewis 8- by 6-Foot Supersonic Wind Tunnel at 2° and 4° angles of attack. This report presents these data and analyzes in detail the spectral noise effects.

APPARATUS AND PROCEDURE

Propeller

A counterrotation propeller model (fig. 1), designated F7-A7, was used for these experiments. The front propeller is nominally 62.2 cm (24.5 in.) in diameter, and the aft propeller is 60.7 cm (23.9 in.) in diameter. Each propeller has eight blades. See table I for the design characteristics. The

propeller was operated at the design Mach number (0.72) and rotational tip speed (238 m/sec; 780 ft/sec) and at blade setting angles of 58.5° on the front propeller and 55.7° on the aft.

Acoustic Measurements

Pressure transducers (fig. 2) were embedded in a plate suspended from the wind tunnel ceiling and were mounted flush in the wind tunnel side wall through the tunnel bleed holes (fig. 1). A plate (fig. 3) able to translate up and down from the tunnel ceiling was positioned 91.4 cm (36 in.) above the tunnel centerline, which was also the propeller centerline at 0° angle of attack. Five transducers (1P to 5P) were installed in the ceiling plate and five (1W to 5W) in the side wall (representing the fuselage) at the angles shown in table II.

The counterrotation propeller was operated with the individual propellers turning at a speed difference of 100 rpm. In this way a good time average could be obtained for the rotating interaction pattern, yet the tones from the two propellers could be included in the same filter band. Narrowband spectra from 0 to 10 000 Hz with a 32-Hz bandwidth were used. In addition, because of the 100-rpm speed differential extremely narrowband spectra could be obtained at each tone to separate the tones from the front and rear propellers. The angle-of-attack effects on noise could thus be determined for each propeller. These spectra were typically 80 Hz wide with a 1/2-Hz bandwidth.

Operating Conditions and Angle-of-Attack Operation

The wind tunnel was operated at an axial Mach number of 0.72 for these experiments, and the propeller was tested at 0°, 2°, 4°, -2°, and -4° angle of attack α. (For positive angles the model was tipped toward the ceiling; for negative angles it was tipped toward the floor.) By testing at both positive and negative angles of attack the noise could be evaluated effectively on all four sides of the propeller by taking measurements on only the ceiling plate and one side wall. That is, the side wall at $\alpha = -2°$ represents the opposite wall from that at $\alpha = 2°$, etc.

The propeller test rig was taken to angle of attack in two steps as shown in figure 4. The test rig was first pivoted about a point on the support strut (fig. 4(a)). This both put the propeller at angle of attack and moved it above the tunnel centerline and aft of its original location. The strut support was translated along its axis to bring the propeller back to the tunnel centerline (fig. 4(b)). However, this changed the propeller's axial position (moved it downstream at positive angles of attack, fig. 4(c)) and thus the angular position of the transducers with respect to it (table II). This angular change was reflected in the data plots. Because the propeller was brought back to the tunnel centerline, the changes in distance from the propeller to the transducers were small. Therefore no distance correction was applied to the noise data.

RESULTS AND DISCUSSION

In a generalized spectrum from a counterrotation propeller (fig. 5(a)) the front propeller (F7) generates a blade passing tone at BPF_1 and harmonics at $2BPF_1$, $3BPF_1$, etc. The aft propeller (A7), turning faster, generates a blade passing tone at BPF_2 and harmonics at $2BPF_2$, $3BPF_2$, etc. Interaction tones are generated at frequencies where the multiples of the blade passing tones are summed (e.g., $BPF_1 + BPF_2$ or $2BPF_1 + BPF_2$). For the particular conditions of this test the two propellers had the same number of blades and were operated at a speed difference of approximately 100 rpm. Therefore for the general 0- to 10 000-Hz spectra (32-Hz bandwidth) the harmonic tones fell into the same narrow band and were not resolved into separate tones (fig. 5(b)). For instance BPF_1 and BPF_2 fell together as one tone, and the tones at $2BPF_1$, $BPF_1 + BPF_2$, and $2BPF_2$ fell together as one tone. The noise values measured in the fundamental and second harmonic bands (32 Hz) for the different angles of attack are listed in table III. Some of the data channels had extraneous electronic "noise" that provided an artificial "floor" on the data. The first two harmonics (BPF and 2BPF) were sufficiently above this floor so that their values were considered accurate. However, beyond 2BPF the propeller tones were too close to this floor and are therefore not reported.

As a result of the intentional 100-rpm difference in speed the separate propeller tones were measurable (as in fig. 4(a)) if a very narrowband (1/2 Hz) spectrum (e.g., fig. 5(c)) was taken about each tone. These results are listed in table IV.

In this section the tones at the blade passing frequencies are discussed first, followed by those at twice the blade passing frequencies. In each group the results for each propeller, taken from the very narrowband spectrum, are discussed first, followed by the total noise measured with the 32-Hz bandwidth.

Tones at Blade Passing Frequencies

Front propeller. - On the ceiling plate the front-propeller noise went down at positive angles of attack (fig. 5(a)) and went up slightly at negative angles of attack (fig. 5(b)). As much as a 7-dB reduction was observed at $\alpha = 4°$ at about the 63° position. The noise reduction at positive angles of attack appeared to be greater than the noise increase at negative angles of attack. (The ceiling at negative angles of attack corresponds to the tunnel floor at positive angles of attack; so at positive angles of attack, the noise on the floor would increase.)

On the tunnel side wall the trend was reversed. At positive angles of attack the front-propeller noise went up, as much as 5 dB (fig. 7(a)) and at negative angles of attack the noise tended to go down (fig. 7(b)). (Note that the forward propeller rotated clockwise as viewed from upstream.) These noise changes are significant and could have a measurable effect on passenger acceptance of advance turboprop aircraft.

Rear propeller. - On the ceiling plate some rear-propeller noise increases were observed with positive angles of attack (fig. 8). These changes were not as strong or well defined as those measured in the front-propeller tones and were in the opposite direction. The front-propeller noise behaved like that of single-rotation propellers (refs. 1 to 3), but the rear-propeller noise exhibited opposite trends.

On the tunnel side wall the rear-propeller blade passing tone did not change much with angle of attack (fig. 9). The noise at both positive and negative angles of attack was about the same.

Simple noise generation model. - A simplified model of the noise generation at angle of attack will aid in interpreting these results. Figure 10(a) shows a propeller operating in a wind tunnel as viewed from upstream. The propeller rotates clockwise, and for these purposes is shown with four blades, one each at positions A, B, C, and D. As the propeller goes to positive angle of attack (fig. 10(b)), the propeller blade's angle of incidence to the flow changes as the blade goes from position to position.

Figure 10(c) illustrates the angle of incidence changes for an individual propeller blade. At position A the lift on the blade would be reduced. At position C, 180° away from position A, the lift would be increased. At positions B and D little change in lift would occur. So in moving from position B to position C the lift would increase to the maximum roughly at position C. Then in moving to position D the lift would decrease to that for $\alpha = 0°$. The lift would decrease further in moving past position D until it exhibited the minimum lift at roughly position A.

These lift fluctuations create noise, which is radiated from the blade and measured by the ceiling plate and side-wall transducers. For this model it is assumed that the generated noise radiates roughly perpendicular to the advancing side of the blade, as confirmed by the results of reference 5 on wing shielding.

If the blade lift responded instantaneously to the velocity fluctuation and radiated the noise, the noise increase would be measured on the surface approximately 90° from the location of the lift increase. In other words increased lift at position C would cause increased noise at position D. Since the lift starts to increase just after position B, the measured noise should show an increase starting just after position C. The maximum lift increase would be at position C, and the maximum noise increase would be 90° away at position D (fig. 11). The direction of rotation in this model is the same as for the front propeller of the counterrotation propeller tested. As observed in the front-propeller blade passing tone section the noise on the ceiling plate decreased at positive angles of attack and increased at negative angles of attack. The increase of ceiling noise at negative angles of attack corresponds to an increase of the floor noise at positive angles of attack. The measured noise then behaved roughly as would be expected from the noise model. However, on the side wall (position C) noise increased at positive angles of attack and decreased at negative angles of attack. So although the measured noise pattern was roughly that expected from the model, it was rotated slightly and may look generally like that shown in figure 12.

This noise pattern rotation could result from the propeller blades' response to velocity changes. An airfoil's lift response to a gust depends on the reduced frequency of the incoming velocity disturbance with respect to the airfoil. The reduced frequency ω is the product of π times the blade chord C divided by the wavelength L of the incoming disturbance, $\omega = \pi C/L$.

Sears (ref. 6) evaluated the lift response of an isolated airfoil to a transverse sinusoidal gust. The response function for an isolated airfoil and the amount of delay are controlled by ω (fig. 13).

The chord on the outer part of the model blade is approximately 5 cm (2 in.). The blade encounters a complete disturbance cycle once every revolution, so the incoming wavelength is approximately the circumference of the propeller tip circle. Because the propeller diameter is approximately 61 cm (24 in.), the calculated reduced frequency ω is approximately 0.1.

Looking at figure 13 and calculating the phase angle from the real axis would indicate that the response should lead the disturbance. Comparing figures 11 and 12 shows that the observed response did lead the instantaneous noise model - by a larger amount than might be suggested by figure 13 although the trends were in the same direction. The front-propeller noise increases at angle of attack were then roughly as expected from the noise model when the blade response was included.

The front propeller of this counterrotation propeller had noise changes similar to those for single-rotation propellers (refs. 1 to 3). In other words it behaved like a single propeller.

The rear propeller rotated in the opposite direction from that shown in figure 10(a). If the rear propeller were operating as a single propeller at positive angle of attack, the lift increase would be at position A, and the expected noise increase for instantaneous response would be on the floor, position D. A noise increase for the aft propeller was, however, measured on the ceiling plate at positive angles of attack, roughly 180° from where it was expected. This shift cannot now be explained except to say that the passage of the disturbance through the front propeller seems to delay the noise response of the rear propeller by roughly half a revolution.

Total tone. - The variation of the total blade passing tone at angle of attack taken from the 32-Hz bandwidth spectrum, where the tones from the two propellers are in the same narrow band, are plotted in figures 14 and 15.

The total blade passing tone measured on the ceiling plate did not change much with angle of attack (fig. 14), only slightly decreasing around 90°. This lack is explained by the individual propeller tones at angle of attack. The front-propeller noise on the ceiling plate decreased at positive angles of attack while the rear-propeller noise increased. The net result was not much change in the total.

The total noise on the tunnel side wall (representing the fuselage) increased with positive angle of attack (fig. 15(a)) - again as the result of changes in the two propeller tones. The rear-propeller noise changed only

slightly while the front-propeller noise increased. The net result was a noise increase on the down-inboard side of the propeller with angle of attack. To minimize angle-of-attack noise on the fuselage, the front propeller should be operated up-inboard with respect to the fuselage.

As is obvious from figures 14 and 15 it would be hard to interpret the measured noise variations with just the total noise spectra. Therefore counterrotation propeller noise data at angle of attack should be taken so that the two rotor tones can be separated. In other words, the propellers should have unequal numbers of blades or unequal speeds.

Tones at Twice Blade Passing Frequencies

Front propeller. - On the ceiling plate the front-propeller tone at twice blade passing frequency went down at positive angles of attack (fig. 16(a)) and went up at negative angles of attack (fig. 16(b)). The same trend was indicated for the blade passing tone on the ceiling plate.

On the tunnel side wall the front-propeller noise trend with angle of attack was not as pronounced (fig. 17). The tone at twice blade passing frequency did not change much at $\alpha = 2°$ but went up at $\alpha = 4°$. The tone also did not change much $\alpha = -2°$ but went down at $\alpha = -4°$. These trends were similar to the blade passing tone results but not as pronounced.

In general the front-propeller tone at twice blade passing frequency behaved like the blade passing tone. The noise generation pattern (fig. 12) for the harmonic is similar to the directivity of the blade passing tone.

Rear propeller. - On the ceiling plate the rear-propeller noise increased at some positions at positive angles of attack (fig. 18(a)). This increase was similar to but not as great as that for the blade passing tone. At negative angles of attack the results were mixed (fig. 18(b)).

On the tunnel side wall there was no clear change in the tone with angle of attack (fig. 19) - again like the blade passing tone results.

Interaction tone at sum of front- and rear-propeller blade passing frequencies. - Not much change in the interaction tone was observed on either the ceiling plate or the side wall (figs. 20 and 21). The interaction tone is thought to be generated by the wakes and vortices of the upstream propeller interacting with the downstream propeller (ref. 7). Here the interaction noise was not greatly affected by operation at angle of attack.

Total tone. - The variation of the total tone at twice blade passing frequency was taken from the 32-Hz bandwidth spectra, where the tones are in the same narrow band. On the ceiling the total tone decreased somewhat at positive angles of attack (fig. 22) - but not nearly as much as the front-propeller tone at twice blade passing frequency (fig. 16) because the rear-propeller tone and the interaction tone were included in the same narrow band.

On the tunnel side wall the total tone measurement gave mixed results (fig. 23). Some noise increase occurred at $\alpha = 4°$, but not much change occurred at negative angles of attack.

The inclusion of all of the tones in one narrow band masked what was happening to each separate tone. As the harmonic number increased and more and more tones were included (fig. 5(a)), the problem became greater. This further emphasizes the importance of taking counterrotation noise data so that the two propeller tones can be separated.

CONCLUDING REMARKS

The noise of a counterrotation propeller at angle of attack was measured in the NASA Lewis 8- by 6-Foot Supersonic Wind Tunnel at cruise conditions. The noise was measured on a plate suspended from the ceiling and on the tunnel side wall. The front and rear propellers had the same number of blades but were operated at a 100-rpm speed difference. This enabled the propeller tones to be separated by using a very narrowband (1/2 Hz) analysis. Total noise at each harmonic was obtained by a 32-Hz-bandwidth, 0- to 10 000-Hz-spectra analysis.

The front-propeller blade passing tone decreased on the ceiling plate and increased on the side wall when the propeller went to positive angles of attack. The decrease on the ceiling was as much as 7 dB, and the increase on the side wall (fuselage location) was approximately 4 dB for a down-inboard propeller rotation. The rear-propeller blade passing tone increased on the ceiling plate but showed little change on the side wall at positive angles of attack. The front-propeller noise behaved like that of a single-rotation propeller, but the rear-propeller noise exhibited opposite trends. The noise changes at angle of attack are significant and could measurably affect passenger acceptance of an advanced turboprop aircraft. A simplified model was explored to show how the observed noise patterns might be obtained.

The total noise pattern at the blade passing frequency, taken from the 32-Hz bandwidth spectra, showed little noise change on the ceiling plate and an increase on the side wall at positive angles of attack. The lack of change on the ceiling resulted from adding the front-propeller noise decrease and the rear-propeller noise increase. The increase on the side wall (fuselage location) came from the front-propeller noise increase combined with no change in the rear-propeller noise and implies a preferred airplane configuration. The side-wall total noise increase at positive angles of attack represents what would be measured on the fuselage for a counterrotation propeller with its front propeller rotating down-inboard. The noise for the other side, up-inboard, did not increase and may have decreased slightly. Therefore to minimize the fuselage noise at positive angles of attack, the front propeller of a counterrotation propeller should rotate up-inboard. This would require oppositely rotating propellers on opposite sides of the fuselage.

The total angle-of-attack noise at the blade passing frequency would be very hard to properly interpret without being able to separate the front- and rear-propeller tones. Thus again counterrotation noise data at angle of attack should be taken so that the tones from each propeller can be separated.

The results with the second harmonic (2BPF) tones were similar to the results with the blade passing tone but were not as pronounced. For example, front-propeller tone at twice blade passing frequency decreased on the ceiling plate at positive angles of attack. The interaction tone is thought to be

caused by the upstream blade wakes and vortices striking the downstream propeller. The lack of change at angle of attack indicated that the interaction noise mechanism was probably not being affected by angle-of-attack operation. The total angle-of-attack noise at twice blade passing frequency, being the sum of separate propeller tones and the interaction tone, would be hard to interpret by itself. This further emphasizes the need to be able to separate the rotor tones in order to interpret the data correctly.

REFERENCES

1. Tanna, H.K.; Burrin, R.H.; and Plumbee, H.E., Jr.: Installation Effects on Propeller Noise. J. Aircr., vol. 18, no. 4, Apr. 1981, pp. 303-309.

2. Dittmar, J.H.; and Jeracki, R.J.: Noise of the SR-3 Propeller Model at 2° and 4° Angles of Attack. NASA TM-82738, 1981.

3. Dittmar, J.H.; Stefko, G.L.; and Jeracki, R.J.: Noise of the SR-6 Propeller Model at 2° and 4° Angles of Attack. NASA TM-83515, 1983.

4. Block, P.J.W.: Experimental Study of the Effects of Installation on Single- and Counterrotation Propeller Noise. NASA TP-2541, 1986.

5. Dittmar, J.H.: An Experimental Investigation of Reducing Advanced Turboprop Cabin Noise by Wing Shielding. AIAA Paper-86-1966, July 1986.

6. Sears, W.R.: Some Aspects of Nonstationary Airfoil Theory and Its Practical Application. J. Aeronaut. Sci., vol. 8, no. 3, Jan. 1941, pp. 104-108.

7. Dittmar, J.H.: Some Design Philosophy for Reducing the Community Noise of Advanced Counterrotation Propellers. NASA TM-87099, 1985.

TABLE I. - DESIGN CHARACTERISTICS OF F7-A7 COUNTERROTATION PROPELLER

Number of blades	[a]8/8
Design cruise Mach number	0.72
Nominal diameter, cm (in.)	62.2(24.5)/60.7(23.9)
Nominal design cruise tip speed, m/sec (ft/sec)	238(780)
Nominal design advance ratio	2.82
Hub-to-tip ratio	0.42
Geometric tip sweep, deg	34/31
Activity factor	150/150
Design power coefficient based on annulus area	4.16

[a]Front propeller/rear propeller.

TABLE II. - TRANSDUCER ANGULAR POSITIONS

Transducer[a]	Propeller angle of attack, α, deg				
	0	2	4	-2	-4
	Angle from propeller test rig centerline axis, deg				
1P	63	58	53	68	73
2P	72	67	62	78	83
3P	90	84	79	95	101
4P	99	94	88	105	110
5P	110	105	99	115	120
1W	63	60	57	66	69
2W	72	69	66	76	79
3W	89	85	82	92	96
4W	99	96	92	103	106
5W	110	107	103	113	116

[a] P denotes plate transducers; W denotes side-wall transducers.

TABLE III. - PROPELLER TONE NOISE FROM 0- to 10 000-Hz SPECTRA

(a) Angle of attack, α, 0°

Transducer[a]	Blade passing frequency	Twice blade passing frequency
	Sound pressure level, dB	
1P	151.5	142.0
2P	155.0	143.0
3P	157.5	148.0
4P	158.5	150.5
5P	159.5	149.0
1W	150.0	140.5
2W	149.0	136.5
3W	153.0	139.5
4W	157.5	143.5
5W	155.5	147.5

(b) Angle of attack, α, 2°

Transducer[a]	Blade passing frequency	Twice blade passing frequency
	Sound pressure level, dB	
1P	148.5	139.5
2P	153.0	142.5
3P	157.5	148.0
4P	156.0	147.5
5P	159.5	146.0
1W	150.0	141.0
2W	152.0	137.0
3W	150.0	135.5
4W	159.0	144.0
5W	158.5	147.0

(c) Angle of attack, α, 4°

1P	146.0	139.5
2P	153.0	141.0
3P	156.0	146.5
4P	154.5	147.0
5P	155.5	148.5
1W	149.5	136.5
2W	151.5	140.5
3W	154.0	142.0
4W	157.5	142.5
5W	159.5	144.0

(d) Angle of attack, α, -2°

1P	153.0	143.5
2P	159.0	149.5
3P	156.5	153.0
4P	159.5	149.0
5P	159.0	152.0
1W	150.5	137.5
2W	148.0	138.0
3W	155.0	143.0
4W	156.5	146.0
5W	154.0	146.5

(e) Angle of attack, α, -4°

1P	157.5	145.0
2P	155.0	150.0
3P	159.5	152.0
4P	160.5	150.5
5P	157.5	147.5
1W	146.5	137.0
2W	150.0	136.5
3W	155.5	144.5
4W	156.0	146.0
5W	155.0	143.5

[a]P denotes plate transducers; W denotes side-wall transducers.

TABLE IV. – PROPELLER TONE NOISE FROM EXTREMELY NARROWBAND SPECTRA

(a) Angle of attack, α, 0°

Transducer[a]	BPF_{F7}	BPF_{A7}	$2BPF_{F7}$	$BPF_{F7} + BPF_{A7}$	$2BPF_{A7}$
1P	147.0	147.5	135.5	127.0	132.0
2P	153.0	146.0	137.0	135.0	128.5
3P	152.0	154.0	145.0	134.0	137.0
4P	155.0	153.5	142.5	129.5	142.0
5P	156.5	155.0	136.0	137.5	144.0
1W	148.5	139.5	133.0	132.5	126.5
2W	145.0	145.5	122.0	126.0	(b)
3W	148.5	149.5	137.0	126.0	124.0
4W	153.5	153.5	139.0	132.5	136.0
5W	151.0	151.5	142.0	136.0	141.0

(b) Angle of attack, α, 2°

Transducer[a]	BPF_{F7}	BPF_{A7}	$2BPF_{F7}$	$BPF_{F7} + BPF_{A7}$	$2BPF_{A7}$
1P	145.0	141.5	130.5	132.0	128.0
2P	147.0	147.0	133.0	131.0	133.0
3P	151.5	154.5	139.0	137.0	142.5
4P	148.0	154.0	137.0	132.0	136.5
5P	154.0	155.5	139.5	132.0	139.0
1W	146.0	145.5	136.0	129.5	131.0
2W	148.0	146.5	123.0	131.0	123.0
3W	148.0	145.0	132.0	118.0	117.0
4W	155.0	154.0	136.5	133.0	137.5
5W	154.0	153.5	142.0	137.0	135.5

(c) Angle of attack, α, 4°

1P	138.0	140.0	129.0	128.0	128.0
2P	139.5	150.5	127.0	128.0	127.5
3P	144.5	154.5	135.0	135.0	139.5
4P	147.0	152.0	137.0	128.5	136.0
5P	151.0	152.5	140.5	135.0	140.5
1W	142.5	146.5	126.5	124.0	127.0
2W	145.5	147.5	127.0	129.5	127.0
3W	150.0	147.0	137.0	123.5	123.0
4W	154.5	152.5	133.0	128.5	135.0
5W	156.0	153.5	136.0	135.0	134.5

(d) Angle of attack, α, -2°

1P	151.0	145.0	137.0	136.0	128.0
2P	155.0	155.5	140.5	133.0	138.0
3P	155.0	147.0	143.0	132.0	147.0
4P	158.0	152.5	138.0	132.0	140.0
5P	155.5	155.5	147.0	135.0	144.0
1W	149.0	140.0	127.5	128.0	124.5
2W	145.0	142.0	126.0	128.0	127.0
3W	150.5	151.0	140.5	125.0	132.0
4W	152.5	153.0	141.0	133.0	137.0
5W	151.5	148.5	134.0	134.5	140.0

(e) Angle of attack, α, -4°

1P	155.0	154.0	139.0	138.0	136.5
2P	152.5	149.5	147.5	132.0	136.5
3P	158.0	151.0	143.0	135.0	145.5
4P	158.0	155.5	139.0	137.0	140.0
5P	150.5	155.0	146.0	137.0	136.0
1W	141.0	140.5	128.0	126.0	123.0
2W	144.0	144.0	125.5	124.0	122.0
3W	148.5	153.0	142.0	127.0	135.0
4W	152.5	151.5	141.0	136.0	138.0
5W	150.0	151.5	128.0	130.0	137.0

[a]P denotes plate transducers; W denotes side-wall transducers.
[b]Not visible from tunnel background.

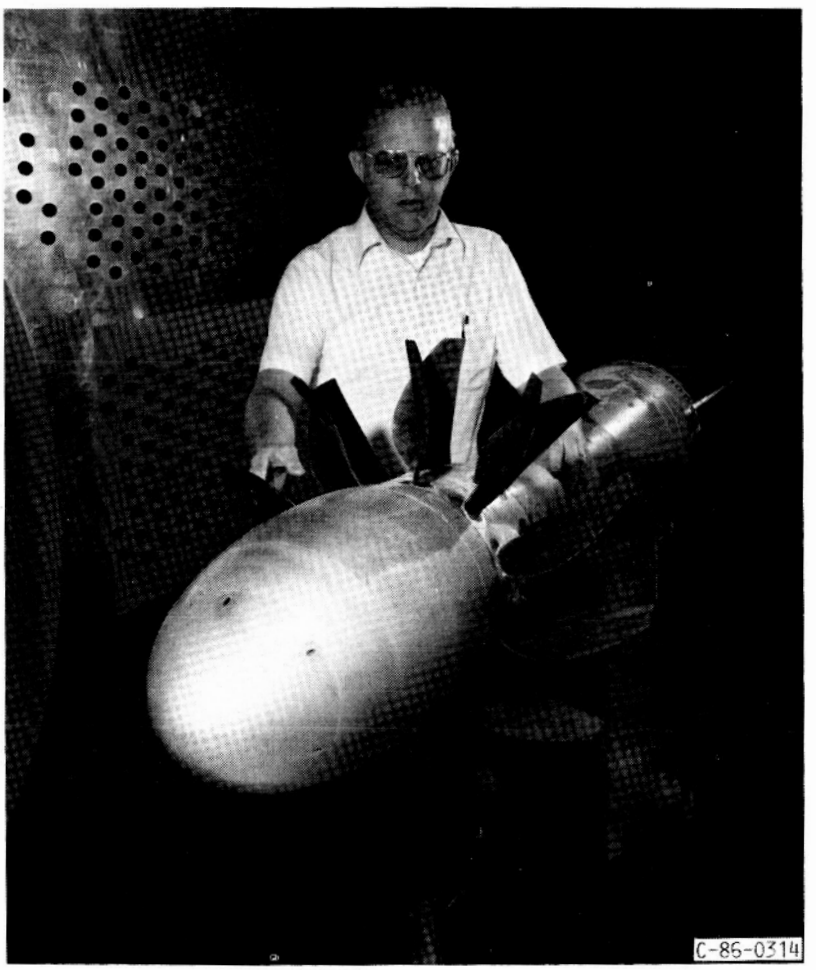

FIGURE 1. - F7-A7 PROPELLER IN WIND TUNNEL.

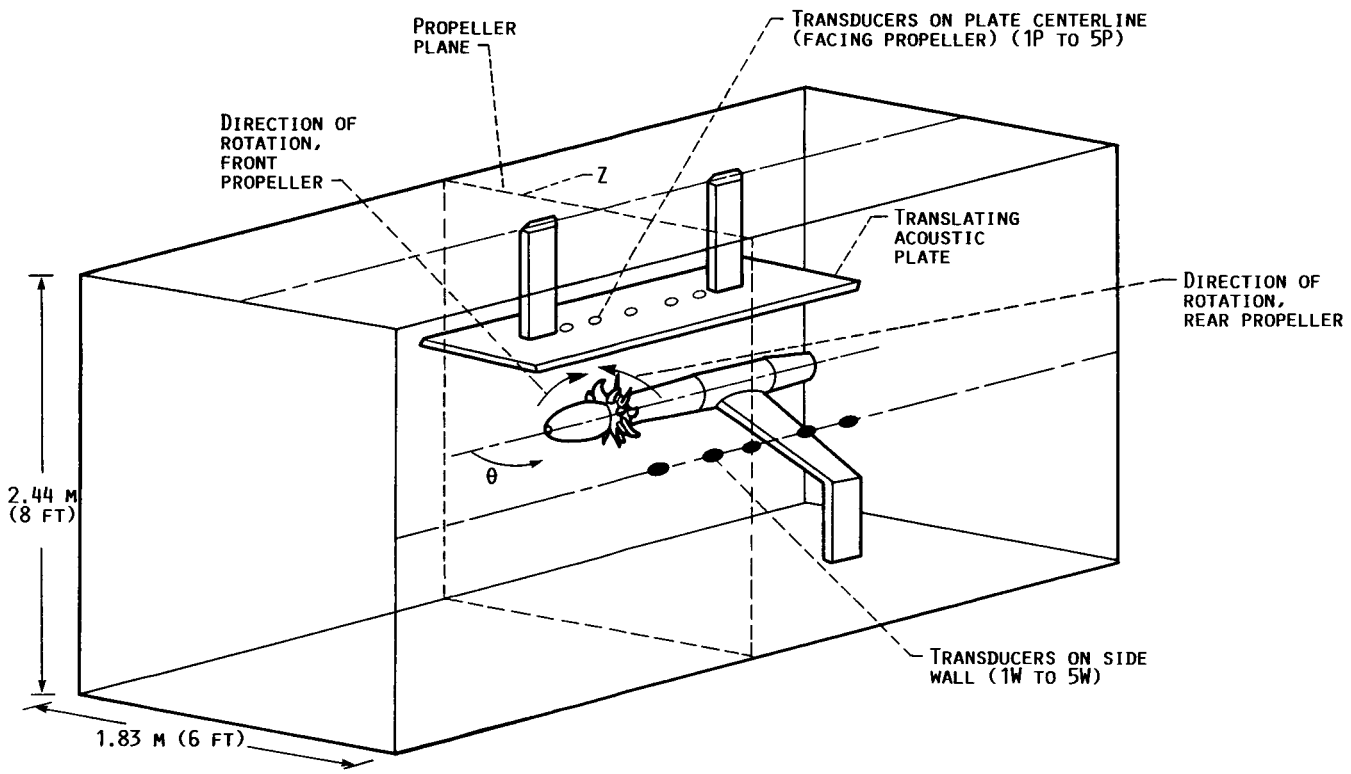

FIGURE 2. - PRESSURE TRANSDUCER POSITIONS.

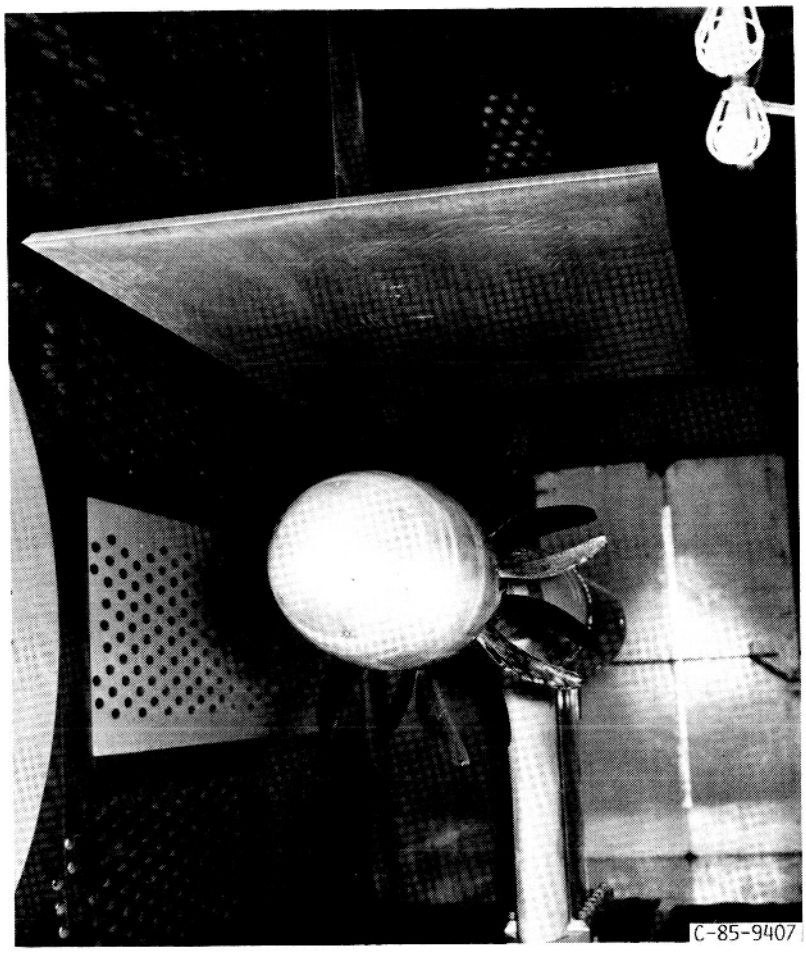

FIGURE 3. - TRANSLATING ACOUSTIC PLATE SUSPENDED FROM WIND TUNNEL CEILING.

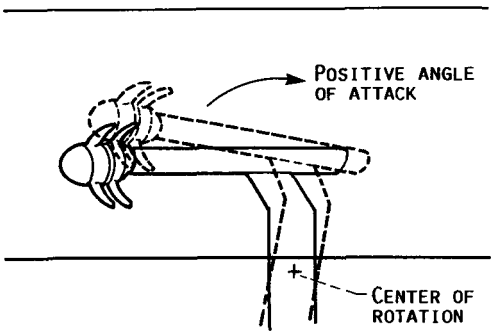

(A) TEST RIG ROTATES ABOUT POINT BELOW TUNNEL WALL.

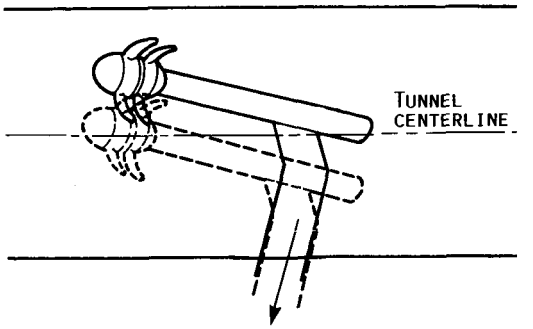

(B) TEST RIG TRANSLATES ALONG STRUT AXIS TO TUNNEL CENTERLINE.

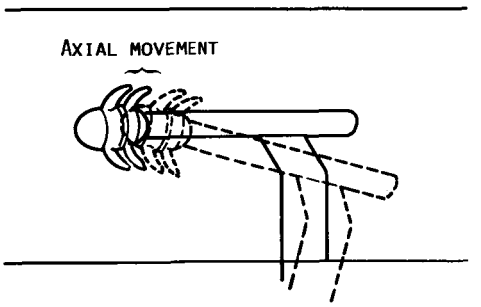

(C) PROPELLER AT ANGLE OF ATTACK HAS ITS CENTER DISPLACED AXIALLY IN TUNNEL.

FIGURE 4. - ANGLE-OF-ATTACK OPERATION.

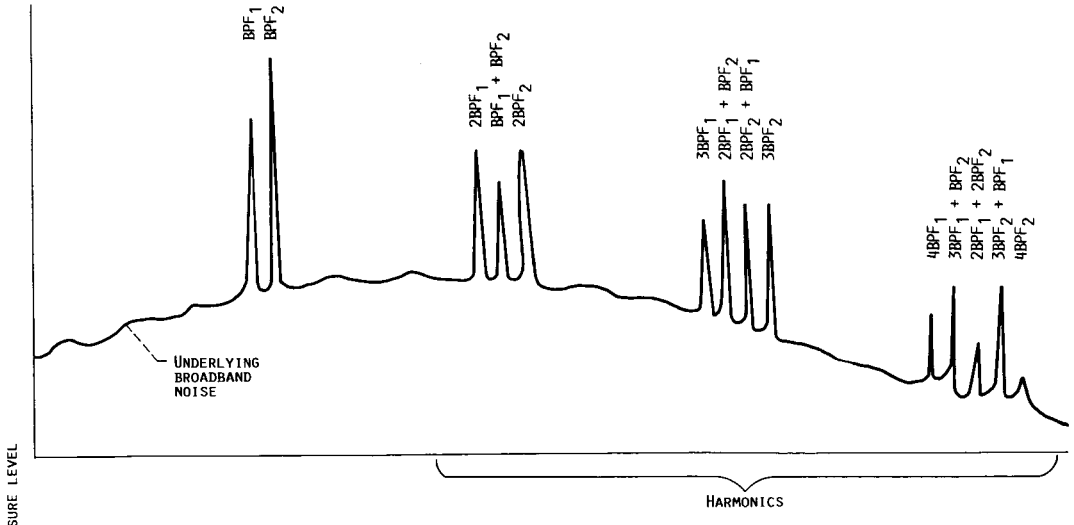

(A) GENERAL COUNTERROTATING PROPELLER NOISE SPECTRUM. (BPF_1 DENOTES BLADE PASSING FREQUENCY OF PROPELLER 1; BPF_2 DENOTES BLADE PASSING FREQUENCY OF PROPELLER 2.)

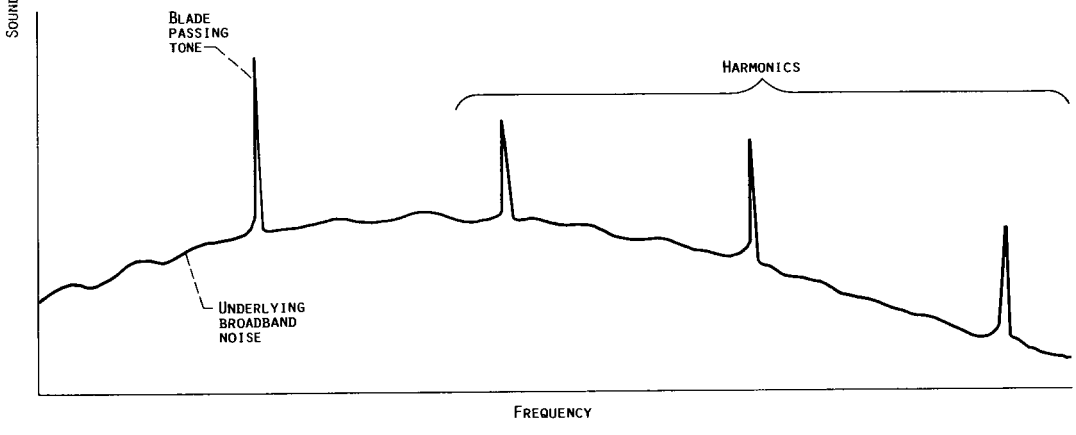

(B) SPECTRUM WITH EQUAL NUMBER OF BLADES AND EQUAL SPEED.

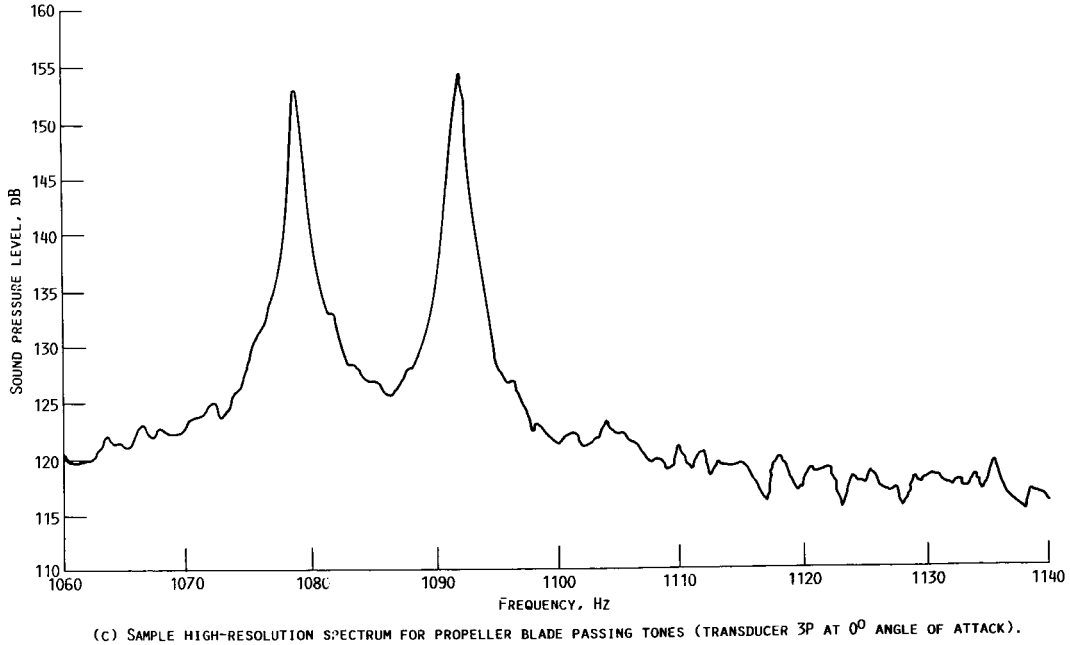

(C) SAMPLE HIGH-RESOLUTION SPECTRUM FOR PROPELLER BLADE PASSING TONES (TRANSDUCER 3P AT 0^{o} ANGLE OF ATTACK).

FIGURE 5. - NOISE SPECTRA.

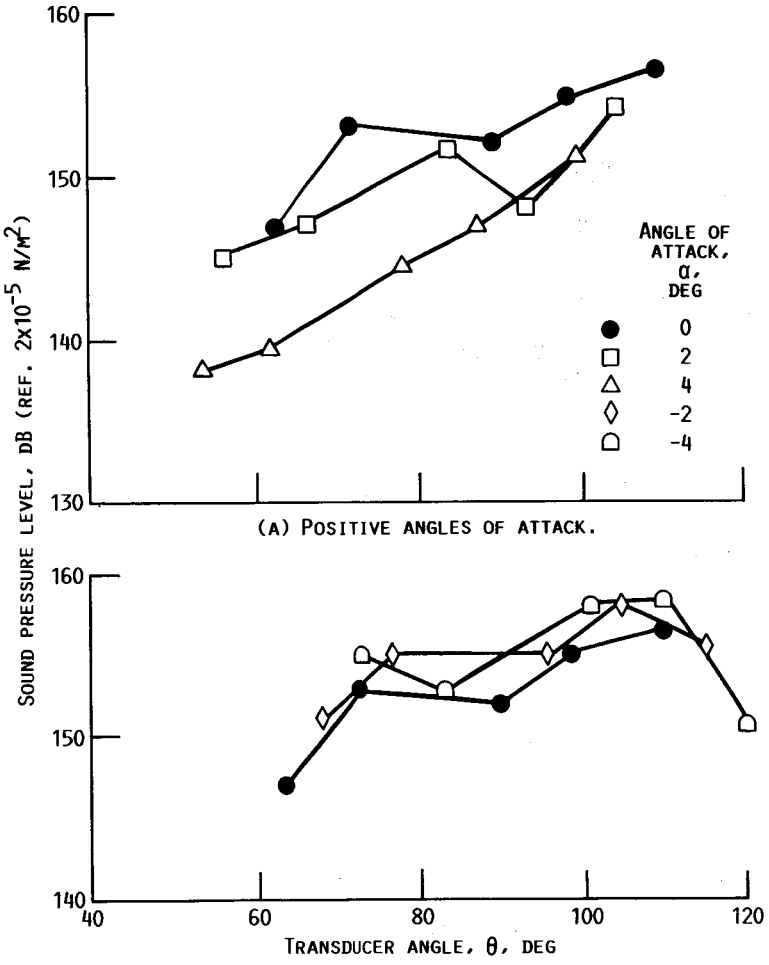

(A) POSITIVE ANGLES OF ATTACK.

(B) NEGATIVE ANGLES OF ATTACK.

FIGURE 6. - BLADE PASSING TONE OF FRONT PROPELLER (F7) ON CEILING PLATE.

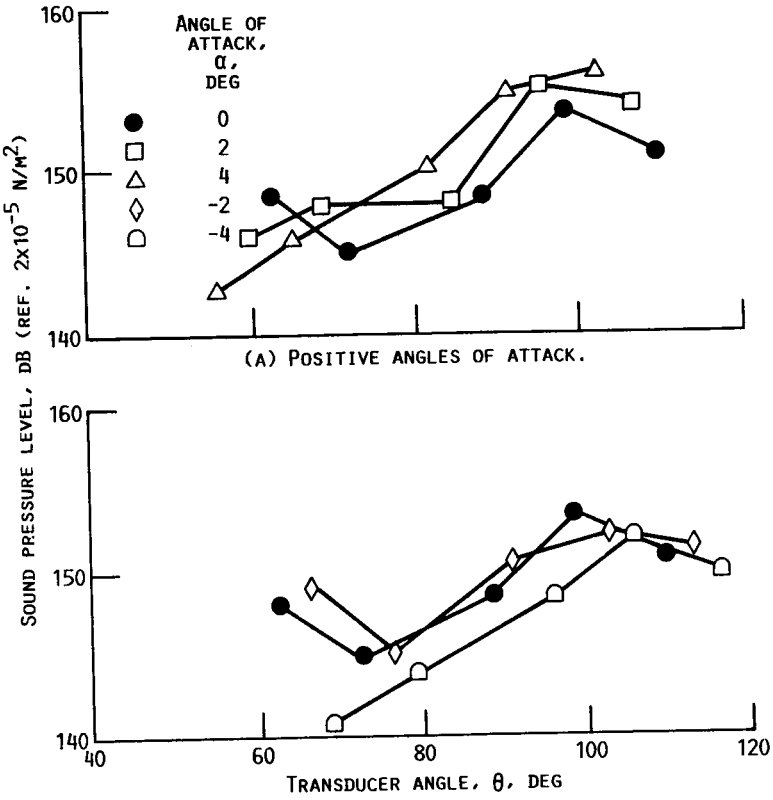

(A) POSITIVE ANGLES OF ATTACK.

(B) NEGATIVE ANGLES OF ATTACK.

FIGURE 7. - BLADE PASSING TONE OF FRONT PROPELLER (F7) ON TUNNEL SIDE WALL.

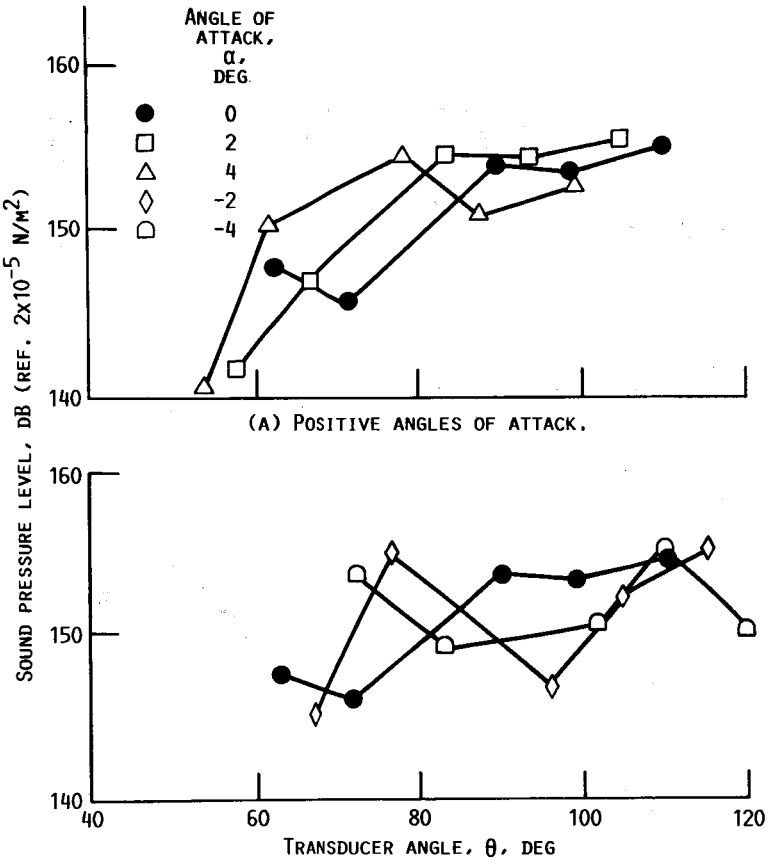

FIGURE 8. - BLADE PASSING TONE OF REAR PROPELLER (A7) ON CEILING PLATE.

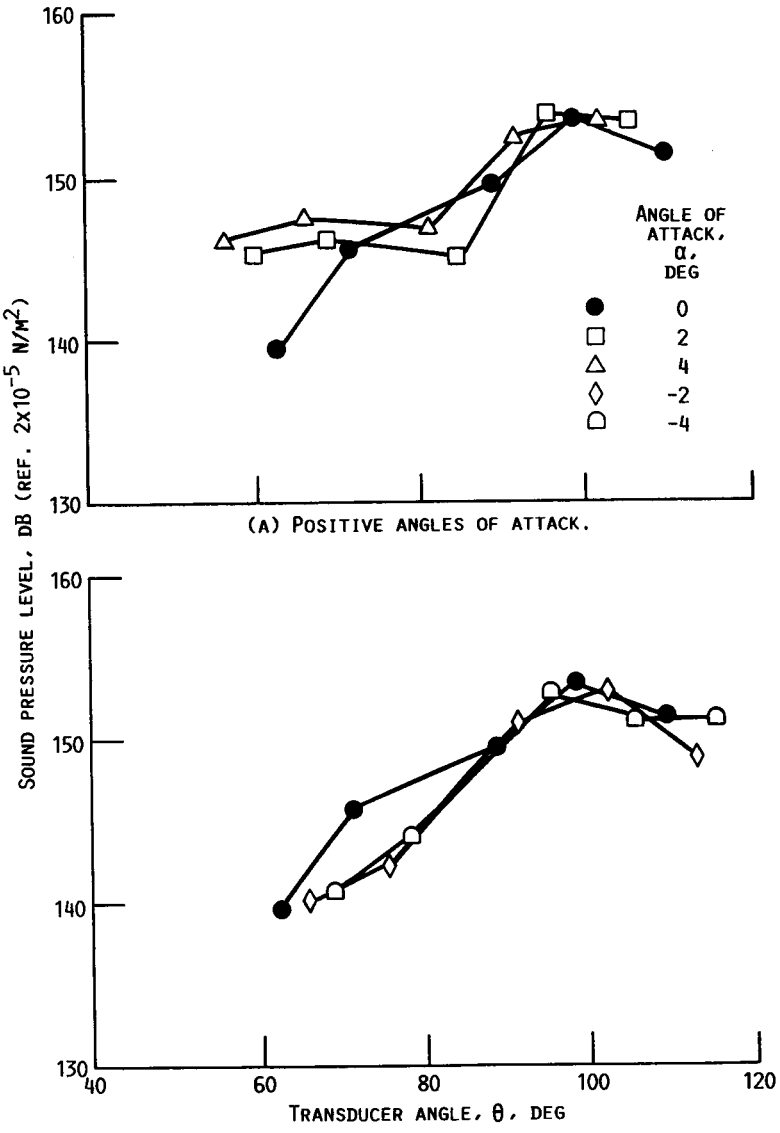

FIGURE 9. - BLADE PASSING TONE OF REAR PROPELLER (A7) ON TUNNEL SIDE WALL.

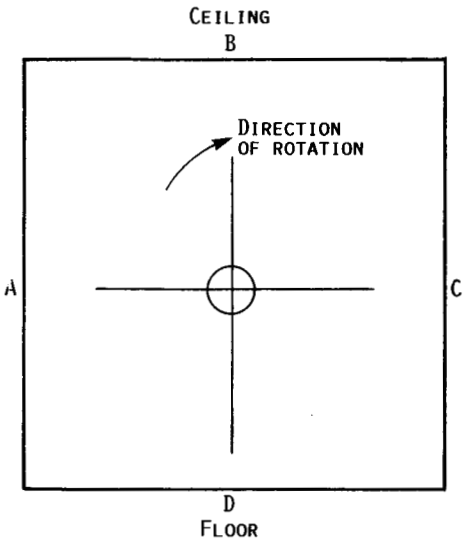

(A) PROPELLER FRONT VIEW.

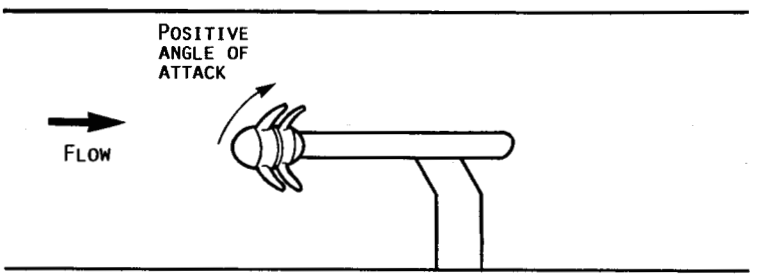

(B) PROPELLER POSITIVE ANGLE-OF-ATTACK DIRECTION.

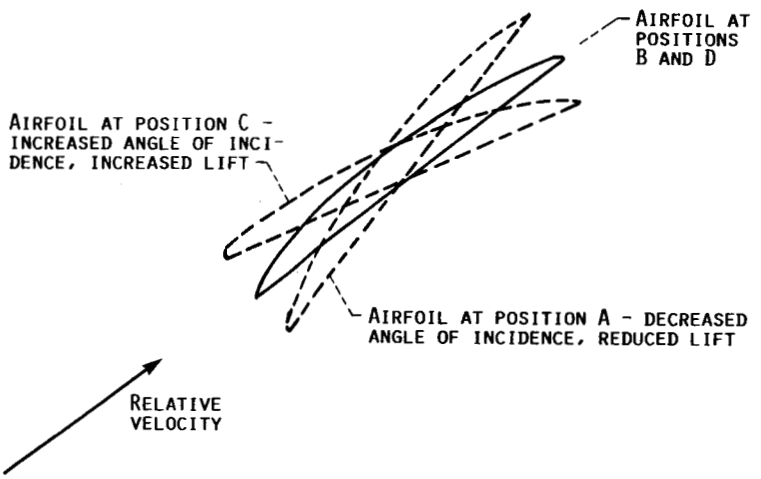

(C) CHANGES IN INCIDENCE ANGLE.

FIGURE 10. - PROPELLER ORIENTATION.

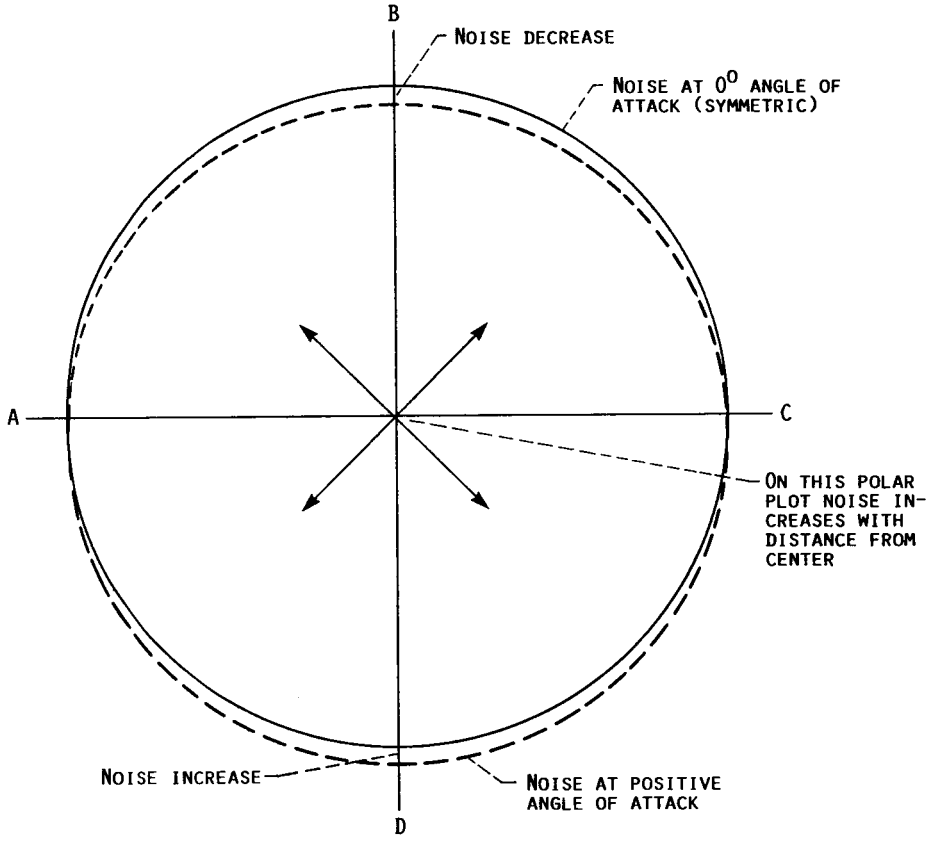

FIGURE 11. - POLAR PLOT OF EXPECTED NOISE AT ANGLE OF ATTACK FOR INSTANTANEOUS RESPONSE.

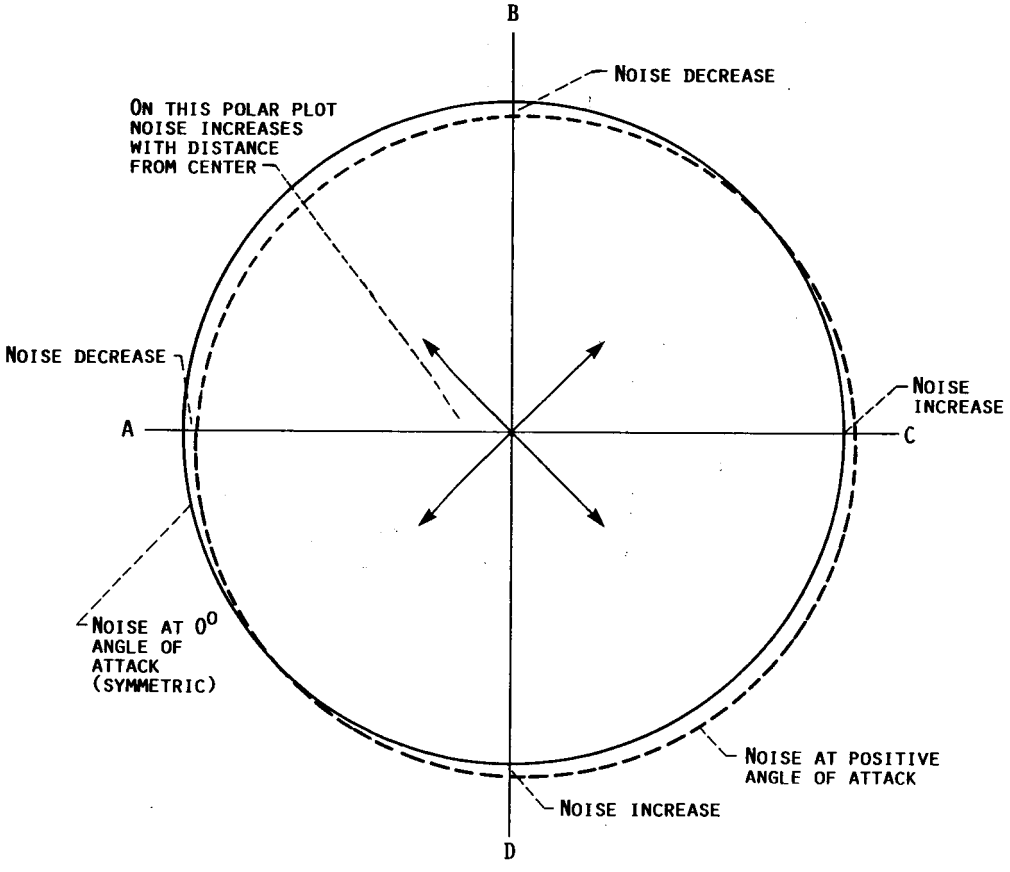

FIGURE 12. - POLAR PLOT OF NOISE AT ANGLE OF ATTACK.

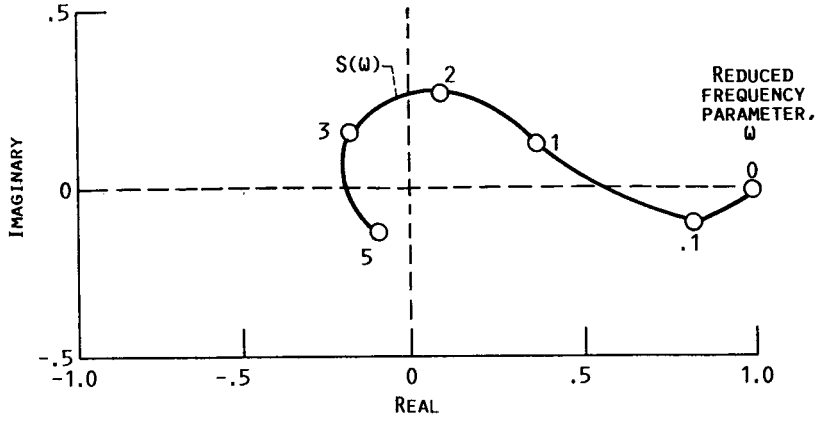

FIGURE 13. - VARIATION OF RESPONSE FUNCTION WITH REDUCED FREQUENCY PARAMETER ω.

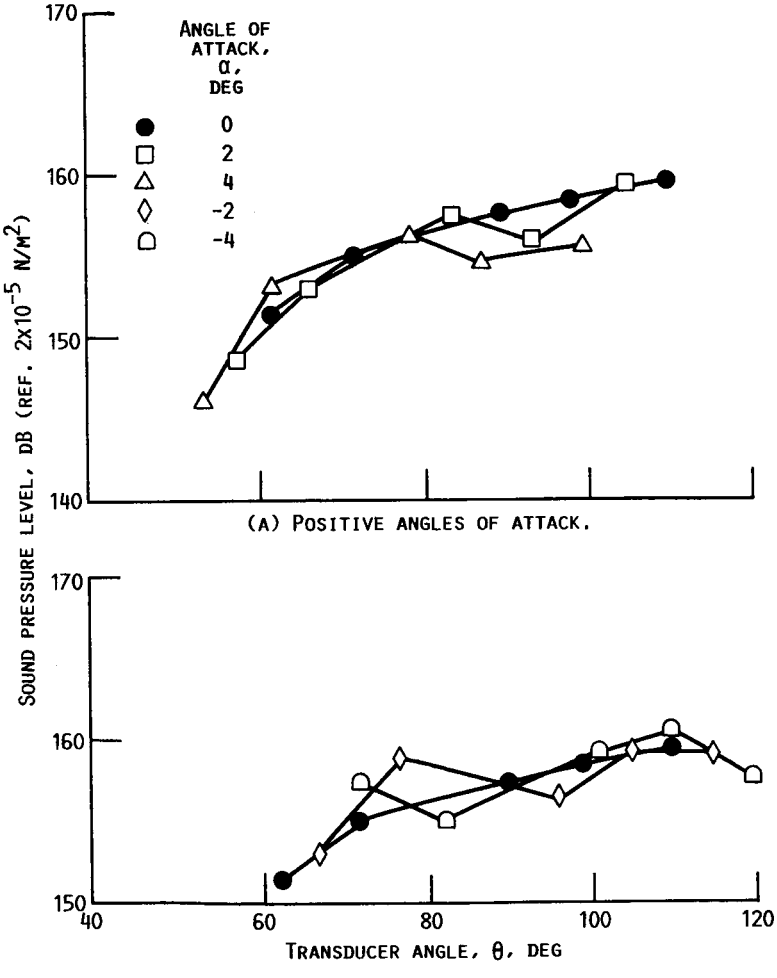

(A) POSITIVE ANGLES OF ATTACK.

(B) NEGATIVE ANGLES OF ATTACK.

FIGURE 14. - TOTAL BLADE PASSING TONE ON CEILING PLATE.

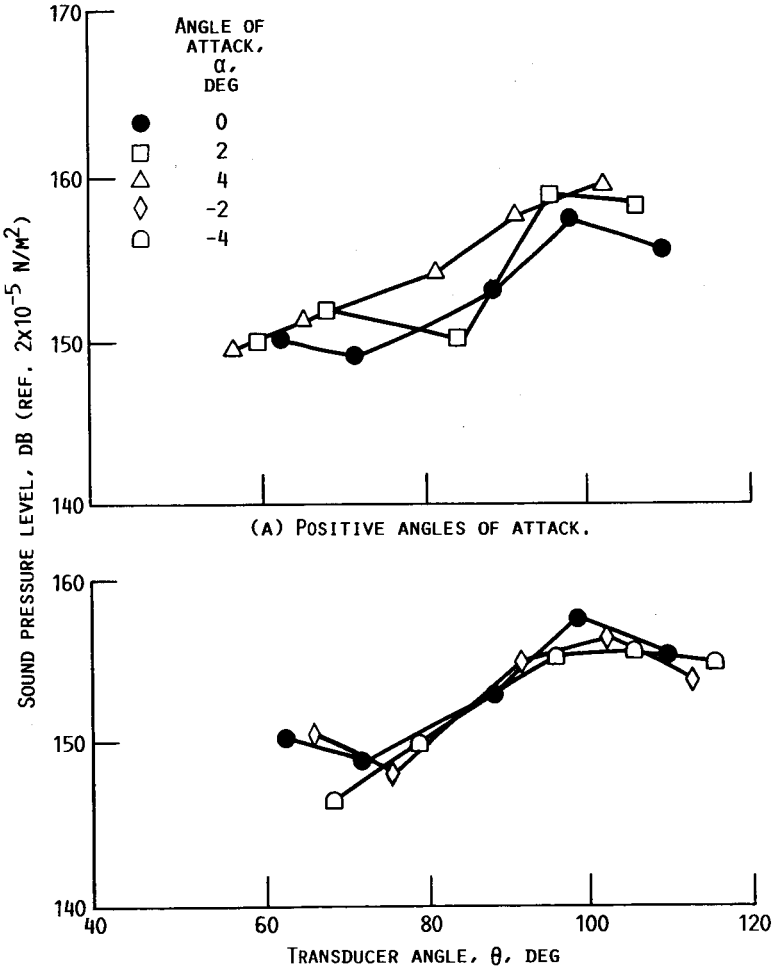

FIGURE 15. - TOTAL BLADE PASSING TONE ON TUNNEL SIDE WALL.

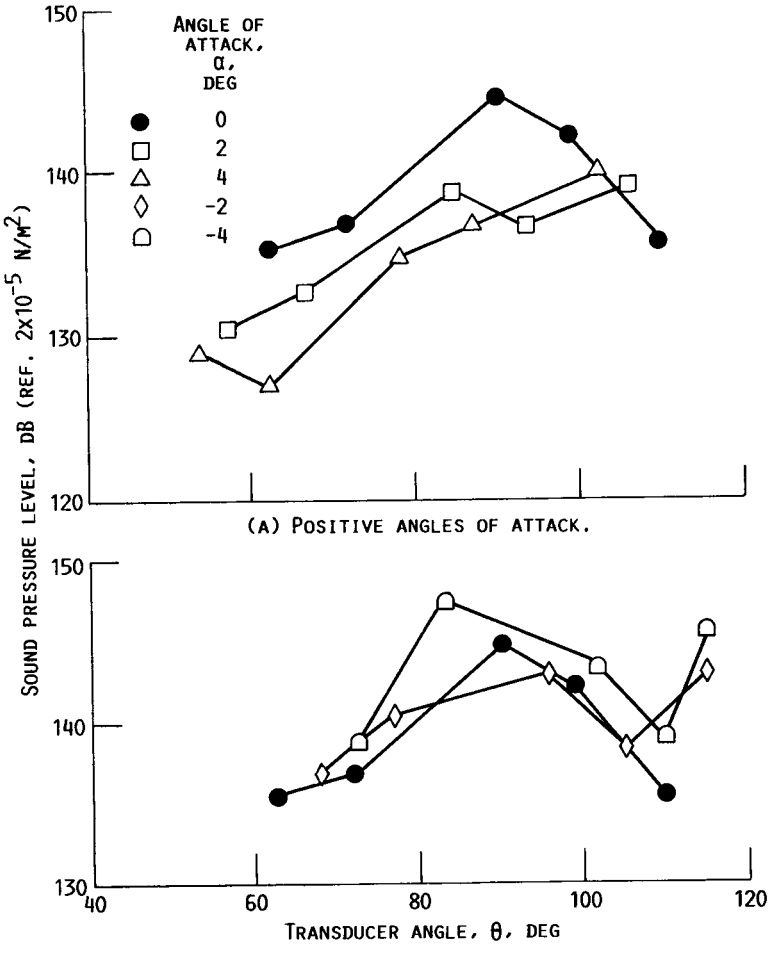

FIGURE 16. - TWICE BLADE PASSING TONE OF FRONT PROPELLER (F7) ON CEILING PLATE.

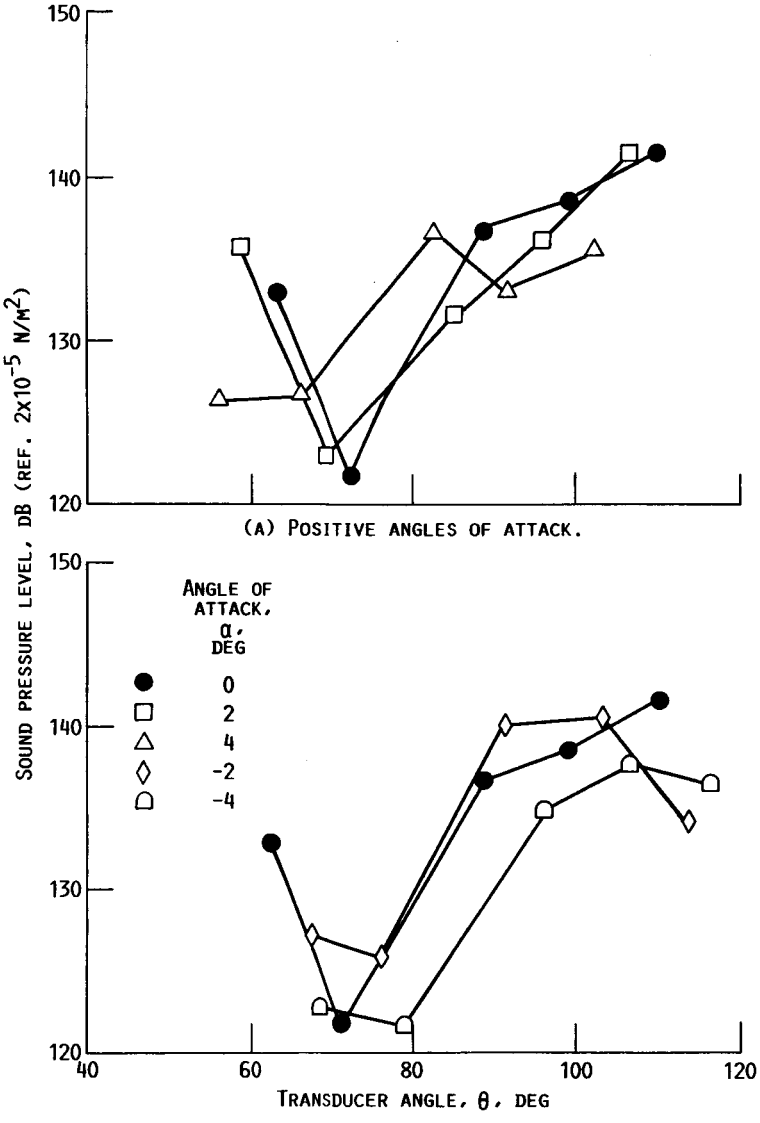

(A) POSITIVE ANGLES OF ATTACK.

(B) NEGATIVE ANGLES OF ATTACK.

FIGURE 17. - TWICE BLADE PASSING TONE OF FRONT PROPELLER (F7) AT TUNNEL SIDE WALL.

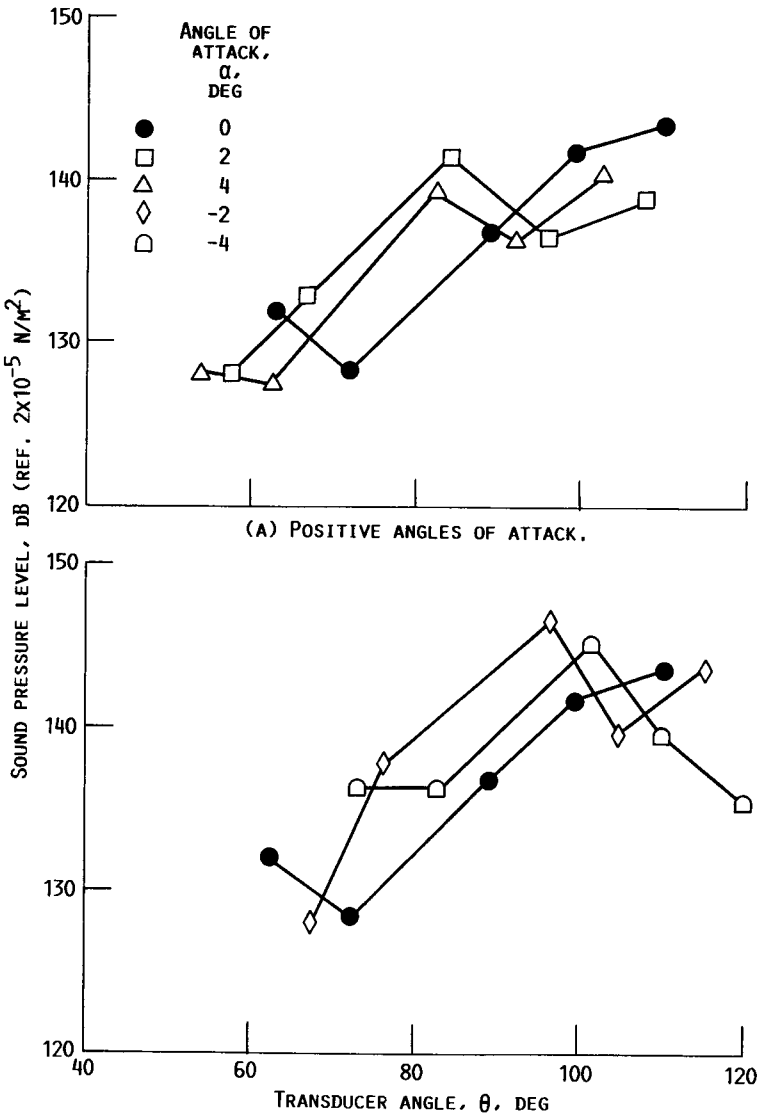

FIGURE 18. - TWICE BLADE PASSING TONE OF REAR PROPELLER (A7) ON CEILING PLATE.

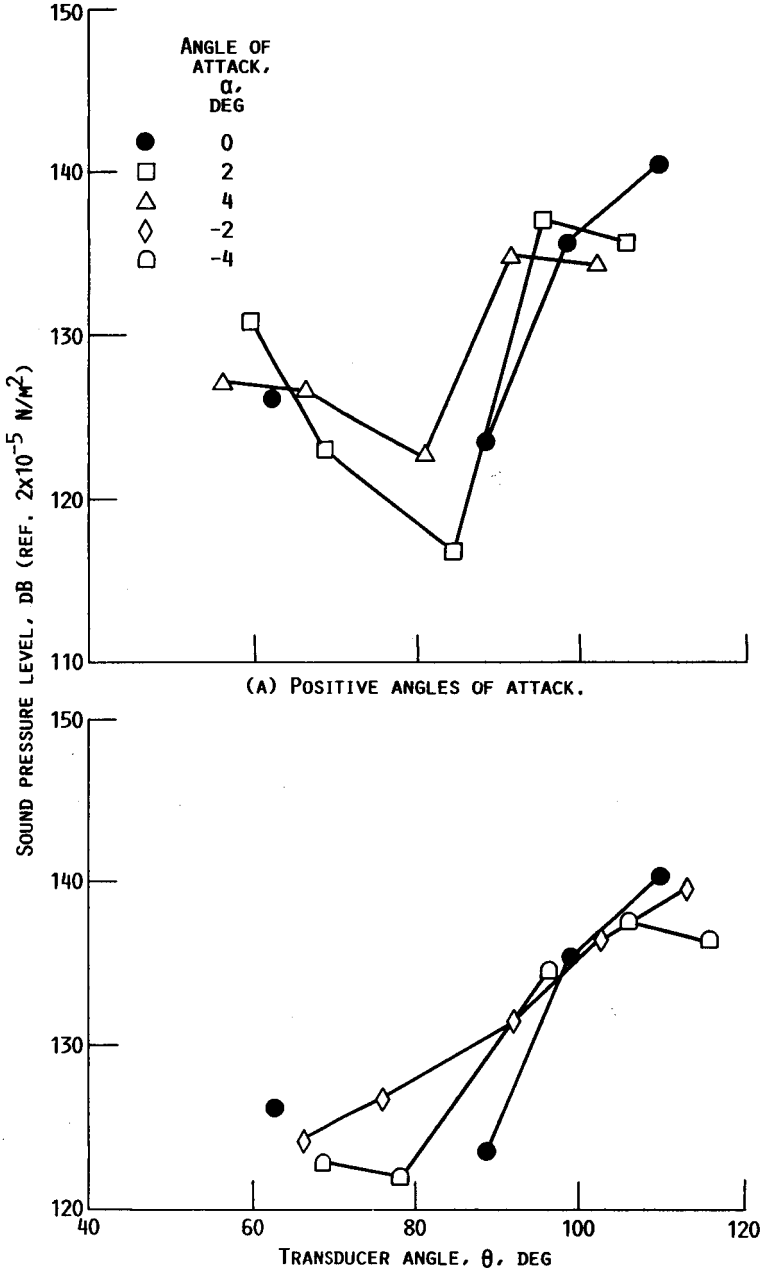

FIGURE 19. - TWICE BLADE PASSING TONE OF REAR PROPELLER (A7) ON TUNNEL SIDE WALL.

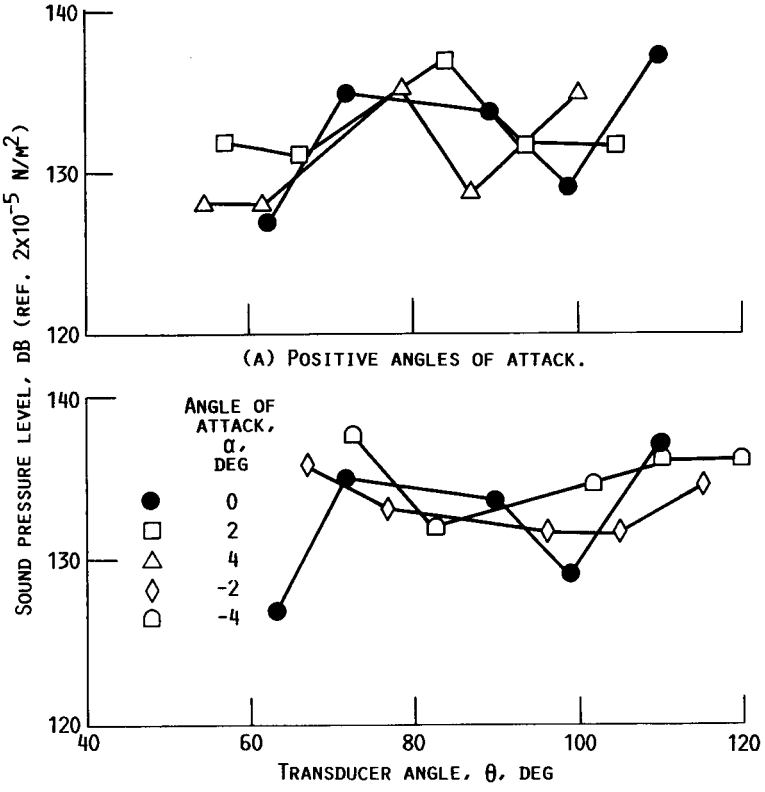

(A) POSITIVE ANGLES OF ATTACK.

(B) NEGATIVE ANGLES OF ATTACK.

FIGURE 20. - INTERACTION TONE AT SUM OF FRONT- AND REAR-PROPELLER BLADE PASSING FREQUENCIES ON CEILING PLATE.

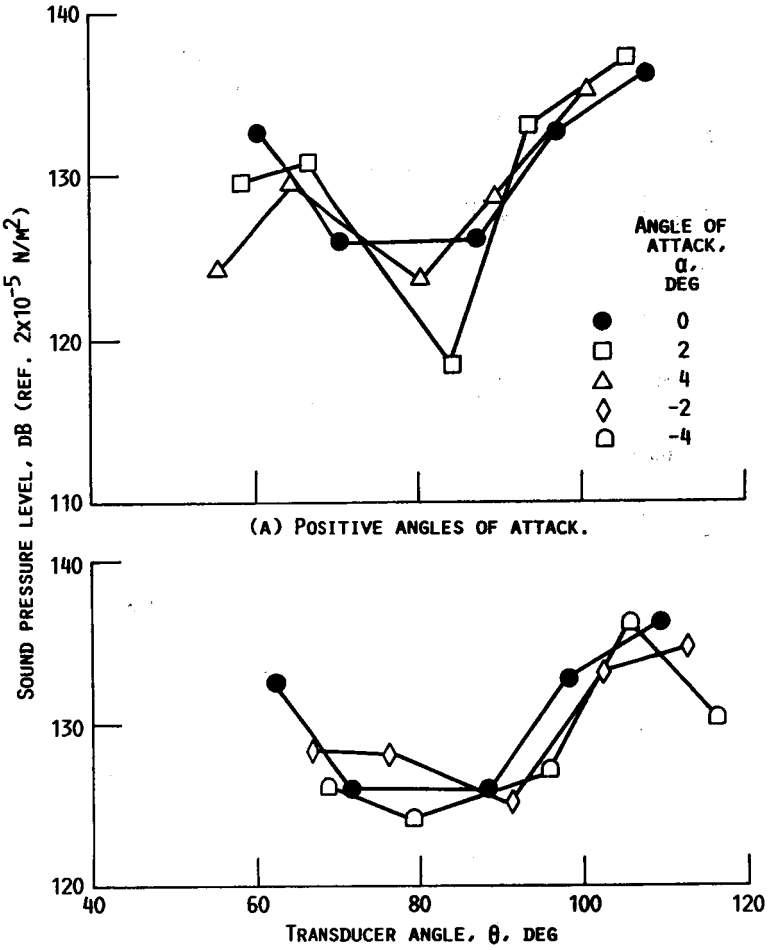

FIGURE 21. - INTERACTION TONE AT SUM OF FRONT- AND REAR-PROPELLER BLADE PASSING FREQUENCIES ON TUNNEL SIDE WALL.

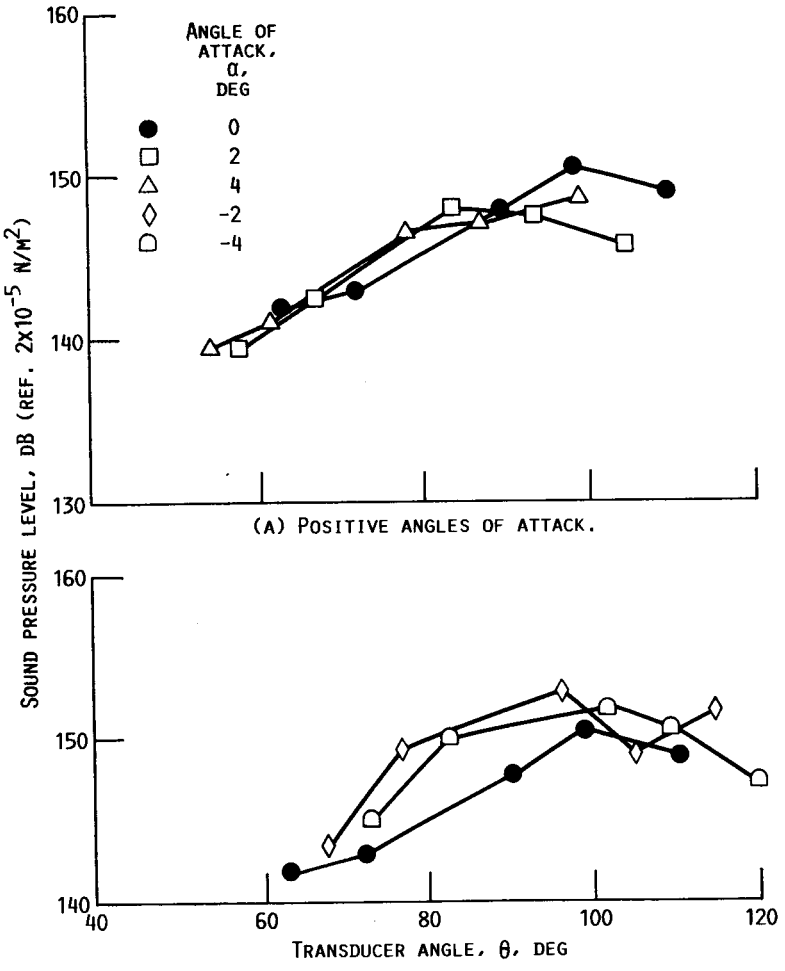

(A) POSITIVE ANGLES OF ATTACK.

(B) NEGATIVE ANGLES OF ATTACK.

FIGURE 22. - TOTAL TONE AT TWICE BLADE PASSING FREQUENCY ON CEILING PLATE.

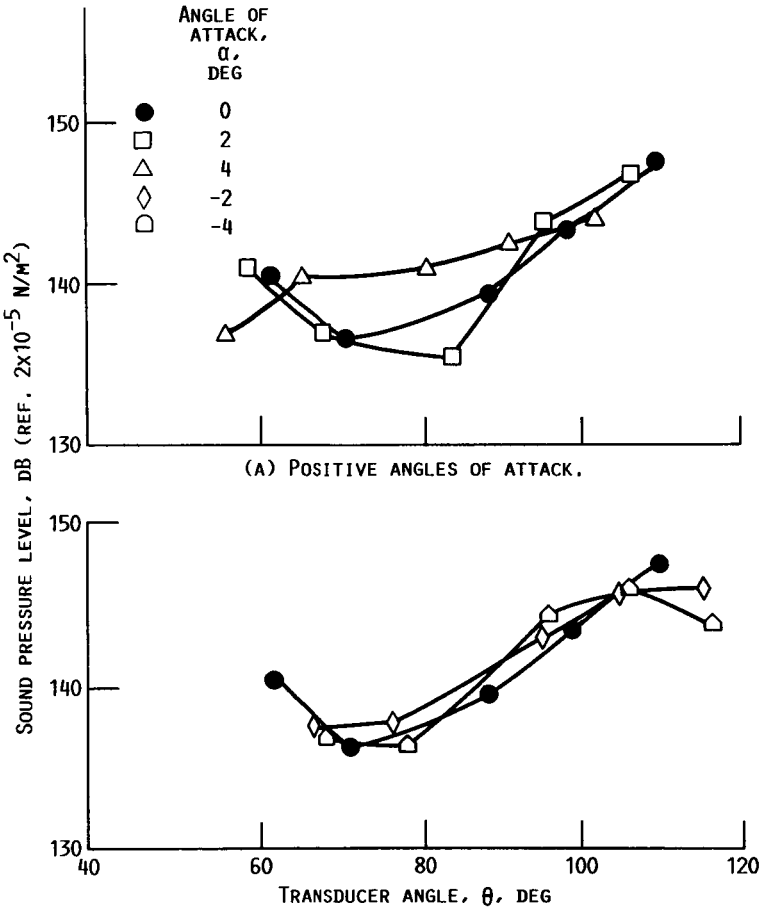

FIGURE 23. - TOTAL TONE AT TWICE BLADE PASSING FREQUENCY ON TUNNEL SIDE WALL.

1. Report No.	2. Government Accession No.	3. Recipient's Catalog No.
NASA TM-88869		

4. Title and Subtitle	5. Report Date
Cruise Noise of Counterrotation Propeller at Angle of Attack in Wind Tunnel	October 1986
	6. Performing Organization Code: 535-03-01
7. Author(s): James H. Dittmar	8. Performing Organization Report No.: E-3275
	10. Work Unit No.
9. Performing Organization Name and Address: National Aeronautics and Space Administration, Lewis Research Center, Cleveland, Ohio 44135	11. Contract or Grant No.
	13. Type of Report and Period Covered: Technical Memorandum
12. Sponsoring Agency Name and Address: National Aeronautics and Space Administration, Washington, D.C. 20546	14. Sponsoring Agency Code

15. Supplementary Notes

16. Abstract

The noise of a counterrotation propeller at angle of attack was measured in the NASA Lewis 8- by 6-Foot Supersonic Wind Tunnel at cruise conditions. Noise increases of as much as 4 dB were measured at positive angles of attack on the tunnel side wall, which represented an airplane fuselage. These noise increases could be minimized or eliminated by operating the counterrotation propeller with the front propeller turning up-inboard. This would require oppositely rotating propellers on opposite sides of the airplane. Noise analyses at different bandwidths enabled the separate front- and rear-propeller tones, as well as the total noise, at each harmonic to be determined. A simplified noise model was explored to show how the observed circumferential noise patterns of the separate propeller tones might have occurred. The total noise pattern, which represented the sum of the front- and rear-propeller tones at a particular harmonic, showed trends that would be hard to interpret without the separate-tone results. Therefore it is important that counterrotation angle-of-attack noise data be taken in such a manner that the front- and rear-propeller tones can be separated.

17. Key Words (Suggested by Author(s))	18. Distribution Statement
Propeller noise; Counterrotation; Angle of attack	Unclassified - unlimited STAR Category 71

19. Security Classif. (of this report)	20. Security Classif. (of this page)	21. No. of pages	22. Price*
Unclassified	Unclassified		

*For sale by the National Technical Information Service, Springfield, Virginia 22161